OPTIMAL UTILIZATION OF WIND ENERGY FOR DYNAMIC SOARING

by Gottfried Sachs, Alexander Knoll, and Klaus Lesch
Technische Universität München, Germany

Presented at the XXI OSTIV Congress, Wiener-Neustadt, Austria (1989)

Introduction

The possibility of extracting energy from moving air and its utilization for flight has been known for quite a long time. This holds both for vertically and horizontally moving air. The flight technique termed dynamic soaring extracts energy from horizontally moving air, which may be characterized as a non-uniform horizontal wind showing a variation with altitude (wind shear). Whereas, vertically moving air is utilized for the flight of sailplanes as a standard practice, the experience in dynamic soaring is rather limited.

The possibility of such extraction from horizontally moving air was first observed with the flight of birds, but it was also earlier considered as a means for use in the flight of sailplanes. In the meantime, more insight has been gained by a number of theoretical investigations and even by some practical experience (Refs. 1-13).

So far, important results have been achieved proving valuable information and knowledge of the principle characteristics of dynamic soaring flight. Some of the investigations are based on simplified models or give an estimate with the use of energy considerations. Others apply numerical simulation techniques for computing flight profiles.

In this paper, modern mathematical optimization procedures are applied to the problem of maximizing energy extraction from horizontally moving air. Thus, it is possible to determine optimal trajectories without simplifying the modeling of the sailplane, and results which give precise information about the capability of dynamic soaring flight can be achieved.

Nomenclature

a_{ik}	=	coefficient (i=u,v,w;k=1,2,3)
b	=	vector of boundary conditions
C_D	=	drag coefficient
C_L	=	lift coefficient
D	=	drag
E	=	max. lift-to-drag ratio, $E=(C_L/C_D)_{max}$
g	=	acceleration due to gravity
H	=	Hamiltonian
h	=	altitude
J	=	performance criterion
K	=	lift dependent drag factor
L	=	lift
m	=	mass of the airplane
n	=	load factor
p	=	parameter vector
S	=	reference area
t	=	time
U_i	=	control estimate
u	=	control vector
u_{Kg}	=	longitudinal component of the absolute speed vector
V	=	airspeed
V_K	=	absolute speed
V_W	=	wind speed
v_{Kg}	=	lateral component of the absolute speed vector
w_{Kg}	=	vertical component of the absolute speed vector
x	=	state vector
x_g	=	longitudinal coordinate
y_g	=	lateral coordinate
z_g	=	vertical coordinate
γ_a	=	angle between airspeed and horizontal plane
λ	=	Lagrange multiplier
μ_a	=	roll angle (aerodynamic coordinate system)
ϱ	=	air density
χ_a	=	azimuth angle (aerodynamic coordinate system

Modeling Considerations

The speed relationships of a sailplane flying in horizontally moving air are illustrated in Figure 1. The speed vector in relation to the earth as an inertial reference system may be expressed as:

$$\vec{V}_K=(u_{Kg},v_{Kg},w_{Kg})^T \qquad (1)$$

with u_{Kg} and v_{Kg} representing the components in the horizontal plane and w_{Kg} the vertical component.

The airspeed may be written as:

$$\vec{V}=\vec{V}_K-\vec{V}_W \qquad (2)$$

where $\vec{V}_W$ represents the wind speed vector. A wind shear condition shows only a horizontal speed component. By appropriate choice of the coordinate axes, the wind speed can be expressed as:

$$\vec{V}_W=(-V_W,0,0)^T \qquad (3)$$

where V_W is a function of altitude. Thus:

$$\vec{V}=(u_{Kg}+V_W,v_{Kg},w_{Kg})^T$$

$$V=\sqrt{(u_{Kg}+V_W)^2+v^2_{Kg}+w^2_{Kg}} \qquad (4)$$

The angular orientation between the vectors VK and V can be expressed by three Euler angles χ_a, γ_a, μ_a (See Figure 2). The following relations hold:

$$\sin\gamma_a=-\frac{w_{Kg}}{V}$$

$$\tan\chi_a=\frac{v_{Kg}}{u_{Kg}+V_W} \qquad (5)$$

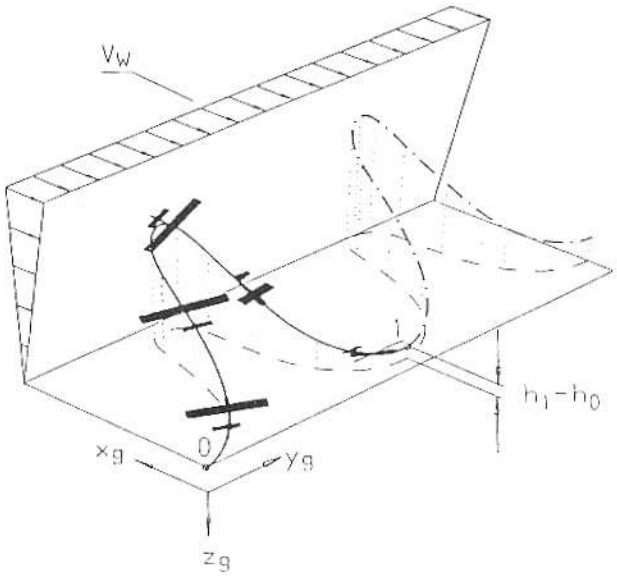

FIGURE 2. BASIC CHARACTERISTICS OF AN OPTIMAL TRAJECTORY FOR DYNAMIC SOARING

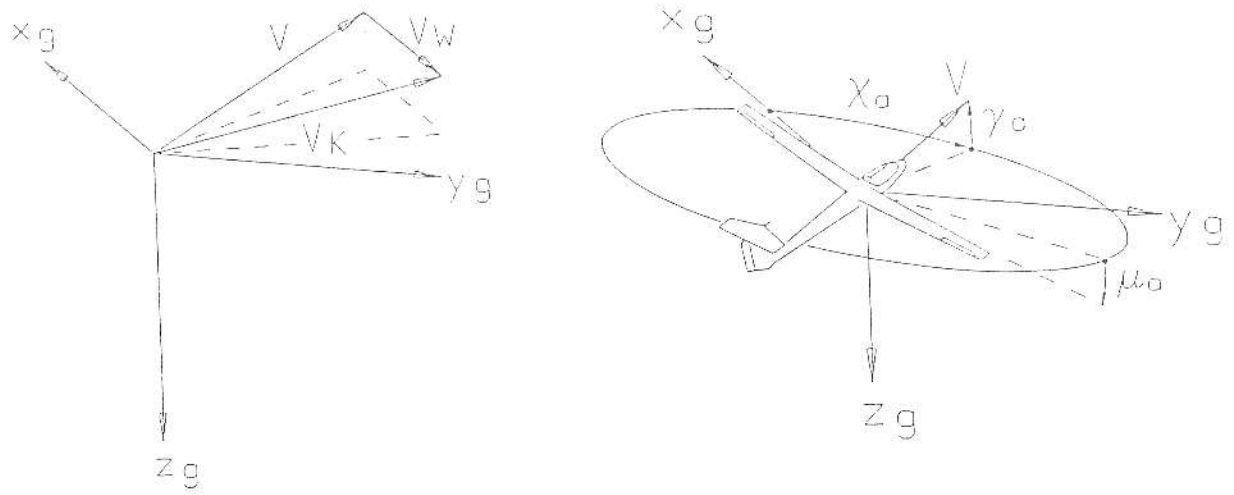

FIGURE 1. COORDINATES, SPEED VECTORS AND ANGLES FOR DESCRIBING THE FLIGHT OF AN AIRPLANE IN HORIZONTALLY MOVING AIR.

The remaining angle μ_a is determined by optimality conditions.

The equations of motion may be written as:

$$\dot{u}_{Kg} = -a_{u1}\frac{D}{m} - a_{u2}\frac{L}{m}$$

$$\dot{v}_{Kg} = -a_{v1}\frac{D}{m} - a_{v2}\frac{L}{m}$$

$$\dot{w}_{Kg} = a_{w1}\frac{D}{m} - a_{w2}\frac{L}{m} + g$$

$$\dot{x}_g = u_{Kg}$$

$$\dot{y}_g = v_{Kg}$$

$$\dot{h} = -w_{Kg} \qquad (6)$$

where

$$a_{u1} = \cos\gamma_a = \cos\chi_a \qquad a_{u2} = \cos\mu_a \sin\gamma_a \cos\chi_a + \sin\mu_a \sin\chi_a$$

$$a_{v1} = \cos\gamma_a \sin\chi_a \qquad a_{v2} = \cos\mu_a \sin\gamma_a \sin\chi_a - \sin\mu_a \cos\chi_a$$

$$a_{w1} = -\sin\gamma_a \qquad a_{w2} = \cos\mu_a \cos\gamma_a$$

The aerodynamic forces are the lift and drag forces denoted by L and D. L is perpendicular to the air speed vector $\vec{V}$ and D is parallel to $\vec{V}$ but opposite to its direction. The aerodynamic forces can be expressed as:

$$D = C_D(\rho/2)V^2S \qquad L = C_L(\rho/2)V^2S \qquad (7)$$

The aerodynamic performance characteristics of the sailplane are determined by its drag polar:

$$C_D = C_{D0} + KC_L^2 \qquad (8)$$

In regard to wind conditions, a linear wind shear model is applied where the gradient dV_W/dh is considered as constant within a prescribed altitude range. This is based on measured data as shown in Figure 2. Furthermore, the wind shear model used as considered as independent of the coordinates x_g and y_g within the region covering an optimal trajectory cycle (the term cycle will be explained subsequently). Figure 3 gives an illustration for the wind shear model applied.

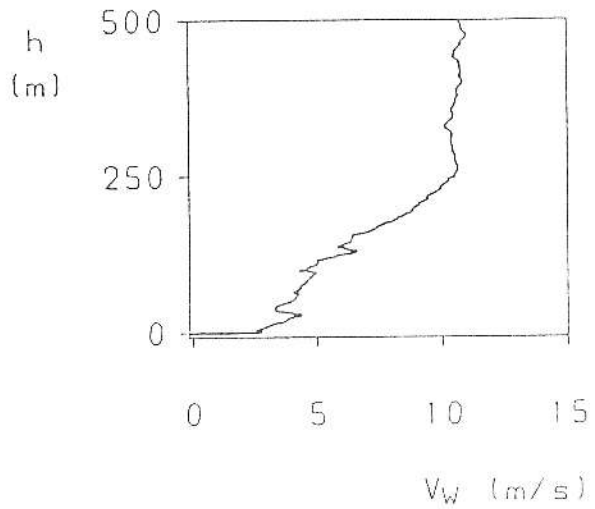

FIGURE 3. WIND SHEAR CONDITIONS (MEASURED DATA, FROM REFERENCE 14)

Basically, an optimal trajectory for maximizing energy transfer to the airplane consists of cycles as shown in Figure 4, with points 0 and 1 denoting the begin and end of a cycle. After completing one cycle, another starts so that the whole trajectory may be considered as a set composed of such individual cycles. The individual cycles may differ, depending on the altitude of the starting point and its wind conditions. No differences exist when the altitude at point 1 is the same as at point 0 ($h_{0\text{-}1} = 0$). In this case, the optimal cycle for soaring flight may be qualified as energy-neutral.

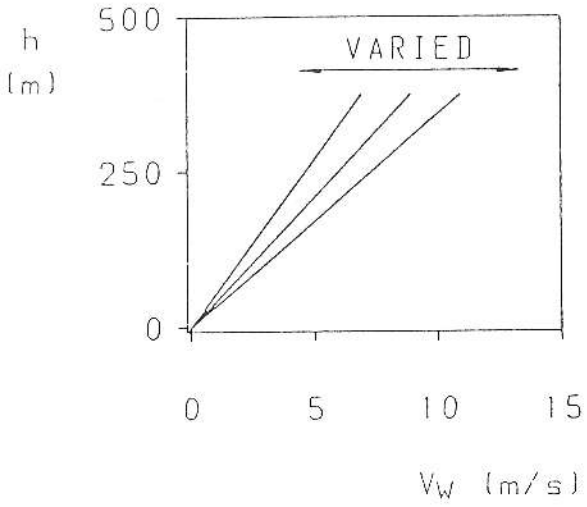

FIGURE 4. WIND MODEL APPLIED

Considering now a cycle as a basic element of an optimal energy-neutral trajectory, the following initial conditions hold (with appropriate choice of the origin of the reference axes):

$$x_g(0) = y_g(0) = 0 \qquad h(0) = h(t_{cyc}), \qquad (9a)$$

where t_{cyc} denotes the time at the end of the cycle.

The speed vector $\vec{V}_K$ at the end of a cycle must be the same as at the beginning. Thus:

$$u_{Kg}(0) = u_{kg}(t_{cyc}) \qquad v_{kg}(0) = v_{kg}(t_{cyc}) \qquad w_{kg}(0) = w_{kg}(t_{cyc}) \qquad (9b)$$

In addition, the initial flight condition can be chosen such that:

$$w_{kg}(0) = 0 \qquad (9c)$$

Control variables are the lift coefficient C_L and the roll angle μ_a. The lift coefficient is subject to the following inequality constraint:

$$C_{Lmin} \le C_L \le C_{Lmax} \qquad (10)$$

Optimization

The optimization problem can now be formulated as to find the controls history (C_L, μ_a), the initial conditions ($u_{Kg}(0)$, $v_{Kg}(0)$) and the cycle length (t_{cyc}) which minimize the performance criterion:

$$J = h(0) - h(t_{cyc}) \qquad (11)$$

with $J = 0$ denoting an energy-neutral trajectory. This problem is subject to the dynamic system described by Eq. (1) and the inequality constraint for the controls according Eq. (10).

The problem described has been solved by applying two optimization programs. One is the optimization program BOUNDSCO which is based on the method of multiple shooting [15,16]. The other is the optimization program TOMP which utilizes a parameterization technique for determining the optimal controls [17]. A short description for both techniques is given in the following.

In regard to the first optimization procedure, necessary optimality conditions according to the minimum principle are applied. Denoting the vectors of the state and control variables by:

$$x(t) = (u_{Kg}, v_{Kg}, w_{Kg}, x_g, y_g, h)^T \qquad (12)$$

$$u(t) = (C_L, \mu_a)^T$$

Eq. (1) can be expressed as:

$$\dot{x} = f(x,u) \qquad (13)$$

Corresponding to the state variables, Lagrange multipliers are introduced

$$\lambda(t) = (\lambda_u, \lambda_v, \lambda_w, \lambda_x, \lambda_y, \lambda_h)^T \qquad (14)$$

The Hamiltonian may now be defined as:

$$H(x, \lambda, u) = \lambda^T f(x, u) \qquad (15)$$

With the use of the Hamiltonian, the Lagrange multipliers are determined by:

$$\dot{\lambda} = -\frac{\partial H}{\partial x} \qquad (16)$$

For the boundary conditions of the Lagrange multipliers, the following relations hold for energy-neutral trajectories:

$$\lambda_i(0) = \lambda_i(t_{cyc}) \qquad i = u, v, w, x, y \qquad (17)$$
$$\lambda_h(t_{cyc}) = -1$$

The optimal controls are such that H is minimized. For this reason, they are determined by:

$$\frac{\partial H}{\partial u} = 0 \qquad (18)$$

or (with regard to C_L) by the constraining bounds of Eq. (10).

The dynamic system described by Eq. (1) is autonomous, so

that the Hamiltonian is constant. Since furthermore the time of a cycle t_{cyc} is considered free, H is given by:

$$H = 0. \qquad (19)$$

As to the second optimization procedure applied, a parameterization technique was used. Here, the control vector $u(t)$ is approximated by a parameter vector p. Defining a grid:

$$0 = t_1 < t_2 < \ldots\ldots < t_{m-1} < t_m = t_{cyc} \qquad (20)$$

the following is applied:

$$u(t) = U_j(p,t),\ t_j \le t \le t_j+1 \qquad (21)$$

The function U_j represents control estimated for interval j, $j = 1,\ldots,m-1$. For modeling the controls, polygonal or spline functions can be applied. For given initial conditions, Eq. (6) can be integrated with the estimated controls and the performance criterion and the boundary conditions can be evaluated. This results in a nonlinear programming problem which may be stated as to minimize the performance criterion:

$$J_p = h_0 - h(p, t_{cyc}) \qquad (22)$$

subject to the boundary conditions:

$$b(p, t_{cyc}) = 0 \qquad (23)$$

Results

In the first part, energy-neutral optimal trajectories are considered. For this type of trajectory illustrated in Figure 5, the potential and kinetic energy at the end of a cycle is the same as at its beginning, including the direction of the speed vector. Thus, the energy extracted from moving air is just sufficient for continuously maintaining dynamic soaring. The geometric

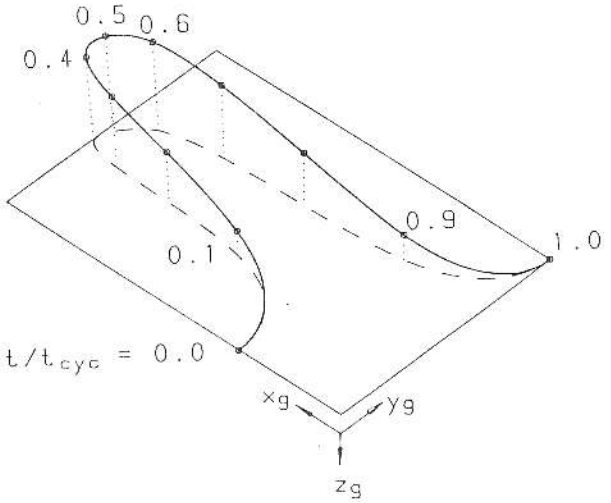

FIGURE 5. ENERGY-NEUTRAL OPTIMAL TRAJECTORY FOR DYNAMIC SOARING (t_{cyc}=29.8 s, E=45, m/S=50 kg/m², dV_W/dh=0.0269^{s-1})

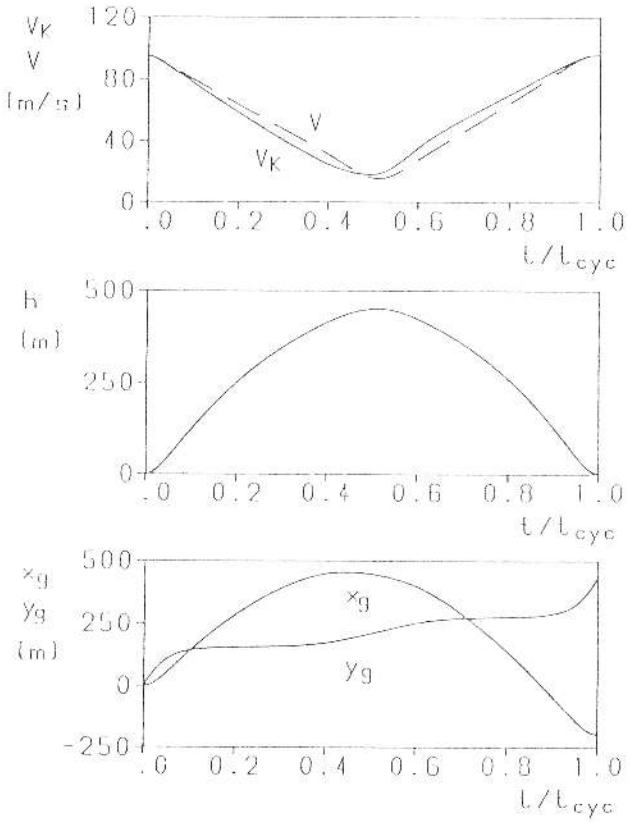

FIGURE 6. STATE VARIABLES OF AN OPTIMAL TRAJECTORY FOR ENERGY-NEUTRAL DYNAMIC SOARING.

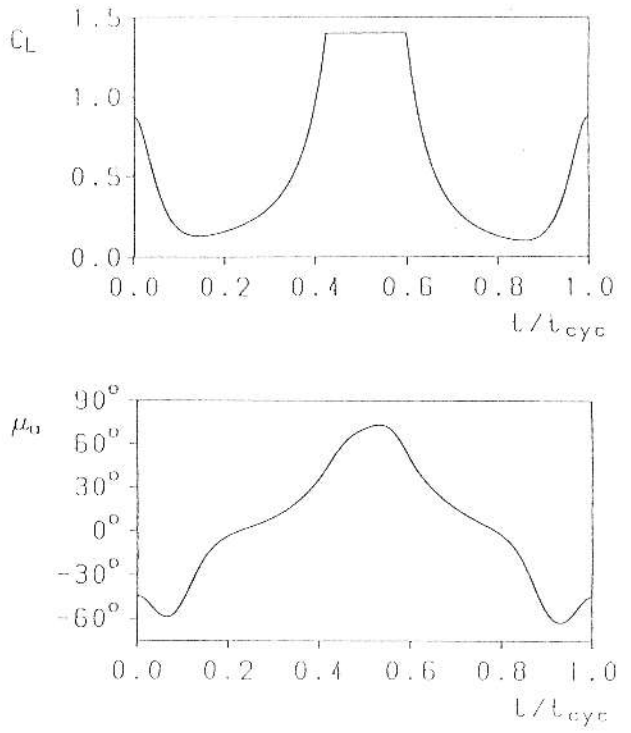

FIGURE 7. CONTROL VARIABLES OF AN OPTIMAL TRAJECTORY FOR ENERGY-NEUTRAL DYNAMIC SOARING

properties of an optimal trajectory show a position change of the airplane, not only crosswise to the wind, but also in its direction.

In Figure 6, the history of state variables is shown. This figure also gives an illustration of the relation between airspeed V and the absolute speed V_K. The controls history is presented in Figure 7. It may be seen that the lifting capability in terms of lift coefficient changes is significantly used. Similarly, large roll angle changes are necessary.

An evaluation of energy-neutral optimal trajectories is presented in Figure 8. This figure shows the minimum wind gradient which is necessary for maintaining dynamic soaring without gaining or losing energy. The minimum wind gradient is plotted as a function of maximum lift-to-drag ratio $E = (C_L/C_D)_{max}$. The results show that maximum lift-to-drag ratio is a key factor as regard the minimum wind gradient necessary. In addition, wing loading m/S exerts a significant influence. In the results presented in Figure 8, the effect of a load factor constraint is also taken into account. The load factor limit considered yields an increase of the wind gradient necessary.

In addition, results for some existing airplanes (the drag polars of which are based on flight test data) are also shown in Figure 8. They are in agreement with the results concerning the quadratic drag polar (Eq. (8)) which is used for systematically investigating the effect of maximum lift-to-drag ratio.

The energy state of the sailplane shows significant changes during the course of an optimal trajectory. This is illustrated in Figure 9. In the first part of the cycle shown, a decrease in the energy state exists. The remaining part shows an increase in the energy state such that the energy extracted from the moving air is greater than the energy detracted by drag work. It may be of interest to note that the most significant energy state increase occurs in the upper part of the trajectory. Additional insight is provided by Figure 10, which shows the rate of change of energy. In this figure, the contribution yielding an energy state

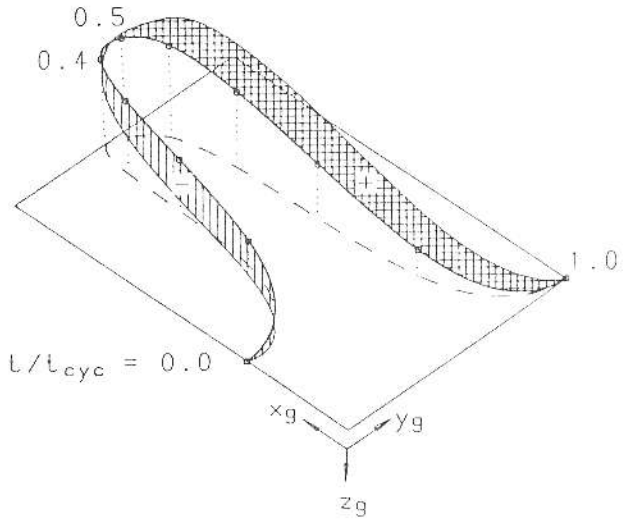

FIGURE 9. CHANGE OF THE ENERGY STATE OF THE AIRPLANE DURING AN OPTIMAL TRAJECTORY

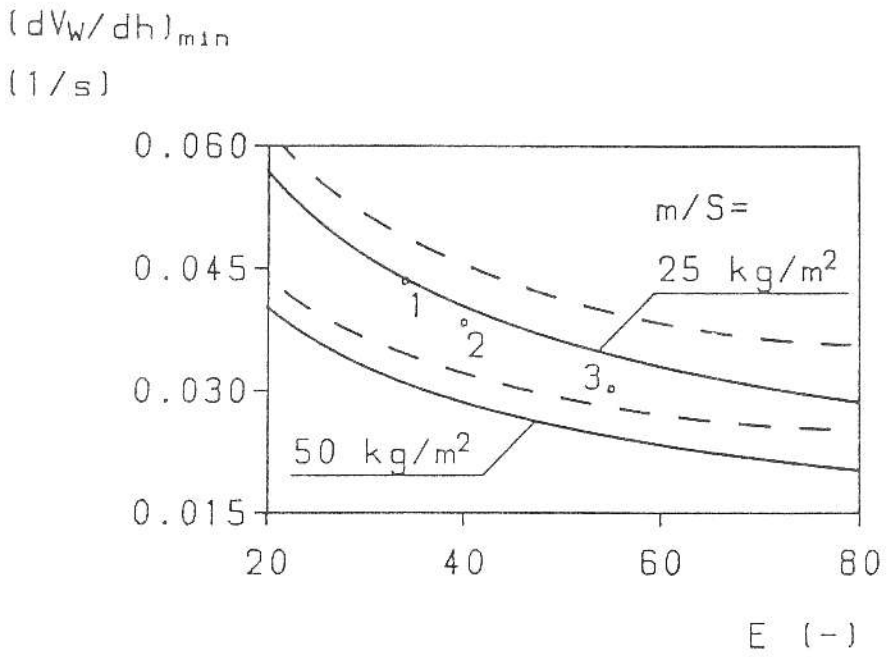

FIGURE 8. MINIMUM SHEAR WIND GRADIENT NECESSARY FOR ENERGY-NEUTRAL DYNAMIC SOARING
-SAILPLANE 1 SIMILAR TO TWIN ASTIR ($M/S = 33.0\ KG/M^2$), CLUB CLASS
-SAILPLANE 2 SIMILAR TO LS 4 ($M/S = 32.2\ KG/M^2$), STANDARD CLASS
-SAILPLANE 3 SIMILAR TO ASW 22 ($M/S = 32.5\ KG/M^2$), OPEN CLASS
DOTTED LINES: LIMITATIONS $V_{MAX} = 90\ M/S$ AND $N_{MAX} = 4.5$

increase due to energy extraction from moving air is compared iwth the contribution detracting energy from the sailplane due to drag work.

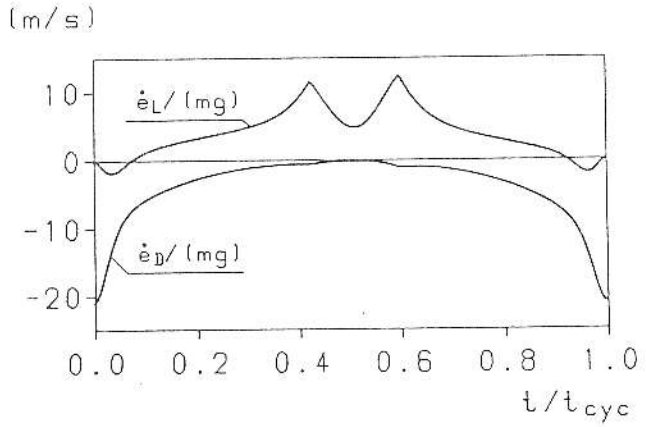

FIGURE 10. RATE OF ENERGY CHANGE (e_L: LIFT CONTRIBUTION, e_D: DRAG CONTRIBUTION)

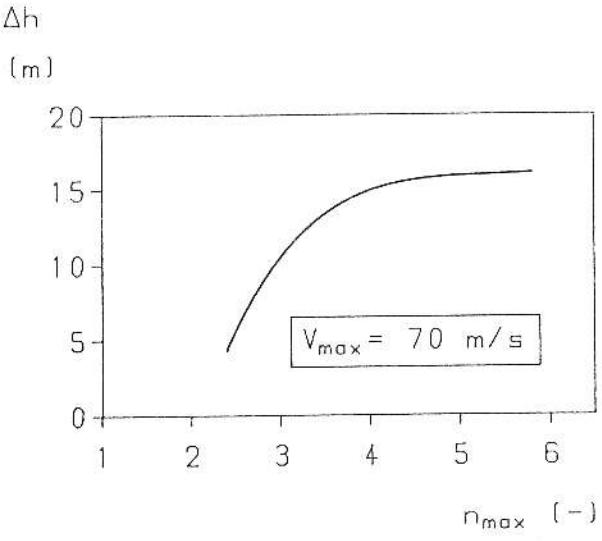

FIGURE 12. ALTITUDE GAIN FOR AN OPTIMAL TRAJECTORY WITH CONSTRAINTS FOR LOAD FACTOR AND AIRSPEED (E = 45, m/S = 50 kg/m², dV_w/dh = 0.039 s⁻¹)

In the remaining part, results are presented for optimal trajectories which show a gain in the energy state after completing a cycle. According to Figure 11, significant gains can be achieved when the wind gradient is greater than the minimum value considered. This figure also shows the peak values of load factor and airspeed which reach rather high levels.

Therefore, it is necessary to account for limits in airspeed and load factor. The effect of such constraints is illustrated in Figure 12, which shows the altitude gain Δh as a function of maximum load factor admissible n_{max} with airspeed limited to V_{max}.

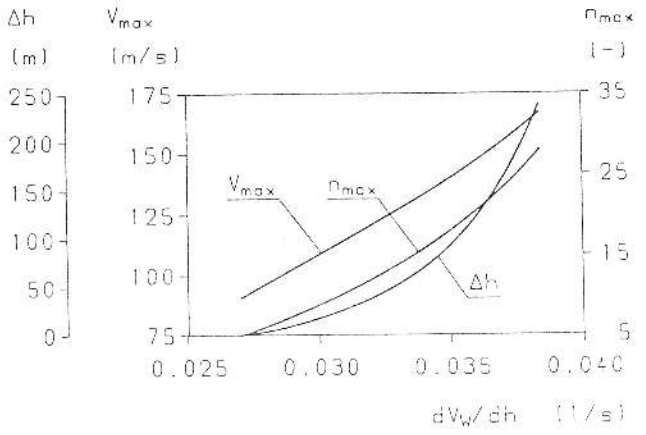

FIGURE 11. ALTITUDE GAIN AND PEAK VALUES OF LOAD FACTOR AND AIRSPEED FOR AN OPTIMAL TRAJECTORY (E=45, m/S = 50 kg/m²)

Conclusions

Modern mathematical optimization procedures are applied for dynamic soaring flight. Thus, flight maneuvers can be determined where the energy extraction from non-uniform horizontal wind (wind shear) and its transfer to the sailplane is maximized.

The minimum wind gradient necessary for continuously maintaining dynamic soaring flight is shown. Maximum lift-to-drag ratio and wing load are key factors as regards minimum wind gradient level. In addition, it is shown what energy gain can be achieved when the wind gradient exceeds the minimum level considered.

References

[1] Prandtl, L.: Beobachtungen uber den dynamischen Segelflug. Zeitschrift fur Flugtechnik und Motorluftschiffahrt, 21. Jahrg. S. 116, 1930.

[2] Idrac, P.: Experimentelle Untersuchungen uber den Segelflug. Oldenbourg-Verlag, Berlin, 1932.

[3] Klemperer, W.: A Review on the Theory of Dynamic Soaring. OSTIC Publication V.

[4] Fritsch, E.: Zum dynamischen Segelflug. OSTIV Publication XI.

[5] Hendriks, F.: Dynamic Soaring in Shear Flow. Dissertation, University of California, Los Angeles, 1972.

[6] Hendriks, F.: Dynamic Soaring in Shear Flow. AIAA Paper No. 74-1003, 1974.

[7] Trommsdorff, W.: Flugmechanische und technische Voraussetzungen fur den Dynamischen Segelflub mit bemannten Fluggerat. OSTIV Publication XIII.

[8] Trommsdorff, W.: Voraussetzeungen fur die Durchfuhrung des dynamischen Segelflugs, Aerokurier, S. 1106-1107, 1976.
[9] Renner, I.: Dynamischer Segelflug. Aerokurier, S. 1104-1105, 1976.
[10] Gorisch, W.: Energy Exchange between a Sailplane and Moving Air Masses under Instationary Flight Conditions with Respect to Dolphis Flight and Dynamic Soaring. OSTIV Publication XIV.
[11] Gorisch, W.: Zum Problem des dynamischen Segelfluges in der horizontalen Grenzschicht zwischen ruhender und bewegter Luftmasse. Aerokurier, S. 855-858, 1977.
[12] Nottebaum, T.: Ein Rechenprogramm zur Simulation des Dynamischen Segelflugs. DGLR-Jahrbuch, S. 329-338, 1987.
[13] Goebel, O.: Scherwindmessungen an Bord einer Piper PA 18 und Auslegung eines Modellsegelflugzeugs fur den Dynamischen Segelflug. DGLR-Jahrbuch, S. 322-328, 1987.
[14] Swolinsky, M.: Beitrage zur Modellierung von Scherwind fur Gefahrdungsuntersuchungen. Dissertation, Technische Universitat Carolo-Wilhelmina, Braunschweiz, 1986.
[15] Bulirsch, R.: Die Mehrzielmethode zur numerischen Losung von nichtlinearen Randwertproblemen und Aufgaben der optimalen Steuerung. Rept. of the Carl-Cranz-Gesellschaft, Oberpfaffenhofen, 1971.
[16] Oberle, H.J.: Numerische Berechnung optimaler Steuerungen von Heizung und Kuhlung fur ein realistisches Sonnenhausmodell. Institut fur Mathematik der Technischen Universitate Munchen, Rept. TUM-M8310, 1983.
[17] Kraft, D.: FORTRAN-Programme zue numerischen Losung optimaler Steuerungsprobleme, DFVLR-Mitteilung 80-03, 1980.